

Radiomics of apparent diffusion coefficient maps to predict histologic grade in squamous cell carcinoma of the tongue and mouth floor: A preliminary study

Jiliang Ren

shanghai ninth peoples hospital

Ying Yuan

shanghai ninth peoples hospital

Meng Qi

shanghai Eye and ENT hospital

Yiqian Shi

shanghai ninth peoples hospital

Xiaofeng Tao (✉ taoxiaofeng_9h@163.com)

shanghai ninth peoples hospital

Research article

Keywords: Head and neck cancer; histologic grade; apparent diffusion coefficient; radiomics; predictor

Posted Date: July 1st, 2019

DOI: <https://doi.org/10.21203/rs.2.10898/v1>

License:   This work is licensed under a Creative Commons Attribution 4.0 International License.

[Read Full License](#)

Version of Record: A version of this preprint was published at Acta Radiologica on June 14th, 2020. See the published version at <https://doi.org/10.1177/0284185120931683>.

Abstract

Background The assessment of histologic grade plays an important part in prognosis evaluation of squamous cell carcinoma (SCC) of the tongue and mouth floor (MF). This study was performed to ascertain if apparent diffusion coefficient (ADC)-based radiomics can predict histologic grade in SCC of the tongue and MF. **Methods** This study involved 95 patients (training cohort: n = 63; testing cohort: n = 32), who were categorized as low- and high-grade SCCs according to the pathologic findings. A total of 526 radiomics features were extracted from ADC maps. Radiomics signature was constructed with least absolute shrinkage and selection operator (LASSO) logistic regression. Receiver operating characteristic curve and area under the curve (AUC) were used to evaluate the performance of the radiomic signature in the training and testing cohorts. **Results** Six features were selected to construct the radiomics signature for predicting histologic grade. The ADC-based radiomics signature performed well in discriminating between low- and high-grade tumors, with AUCs of 0.82 and 0.78 in the training and testing cohorts, respectively. Based on the cutoff value of the training cohort, the radiomics signature achieved accuracies of 0.75 and 0.78, sensitivities of 0.71 and 0.86, and specificities of 0.83 and 0.64 in the training and testing cohorts, respectively. **Conclusions** The ADC-based radiomics signature could identify histologic grade in SCC of the tongue and MF.

Background

Oral and oropharyngeal squamous cell carcinomas (SCCs) are the sixth most common cancer worldwide, nearly half of which arise from the tongue and mouth floor (MF) [1, 2]. Several studies have indicated the association of histologic grade with the prognosis in patients with SCC of the tongue and MF [3-5]. Jerjes et al. [3] revealed that 90% of mortality due to locoregional or distant metastasis occurred in moderately or poorly differentiated (Grade II-III) carcinomas. Therefore, assessment of histologic grade plays an important part in prognosis evaluation SCC of the tongue and MF.

Diffusion-weighted imaging (DWI) with apparent diffusion coefficient (ADC) maps provides a quantitative indicator of water diffusivity, which could reflect information on the microstructure and physiologic state of tissues indirectly. It has been proposed as a potential tool to detect the histologic grade of SCC of the head and neck [6-8]. However, most studies have used the mean ADC value to represent the entire region of interest (ROI) to evaluate histologic grade [6-8]. This approach cannot reflect tumor heterogeneity, and may lead to missing some information on tissues.

Radiomics has attracted increased attention in recent years because medical images contain information about tumor pathophysiology [9]. Radiomics enables the conversion of medical images into high-throughput quantitative features using data-characterization algorithms [10]. The radiomics features extracted from the whole tumor could characterize intratumoral heterogeneity comprehensively, which has profound importance in oncology.[11, 12] Several studies have explored the potential of radiomics to predict tumor-node-metastasis (TNM) stage, status of infection by the human papilloma virus, distant metastasis and survival in patients with SCC of the head and neck [10, 13, 14].

We investigated the value of ADC-based radiomics in SCC of the tongue and MF because we wanted to show that a radiomics signature can be used to identify the histologic grade.

Methods

Patients

The Ethics Review Board of Shanghai Ninth People's Hospital approved the protocol of this retrospective study, and written informed consent was not required. We reviewed medical records from April 2015 to December 2018 to identify patients with SCC of the tongue and MF in our hospital. All patients underwent pretreatment evaluation with DWI magnetic resonance imaging (MRI). The inclusion criteria were: (i) postoperative pathologic confirmation; (ii) no obvious artifact affecting image analyses. Ninety-five consecutive patients (57 men and 38 women; mean age, 55.9 ± 13.4 years) who met the inclusion criteria were identified. We divided the data randomly into the "training cohort" and "testing cohort" via computer-generated random numbers at a ratio of about 2:1. The histologic differentiation of tumors was determined by head and neck pathologists at this single institute. Pathologic reports were made in accordance with WHO (2005) criteria (grade I-III). For statistic purpose, all lesions were divided into low-grade (WHO grade I and I-II), and high-grade (WHO grade II and III).

Image acquisition, image segmentation and radiomics feature extraction

MRI was done on a 3.0-T scanner (Ingenia; Philips Healthcare, Best, Netherlands) by using a head-and-neck array coil. The MRI protocol comprised T1-weighted imaging (T1WI), T2-weighted imaging (T2WI), DWI, and contrast-enhanced T1WI. DWI was undertaken using a single-shot spin-echo echo-planar imaging sequence. The imaging parameters for DWI were: a repetition time of 1922 ms; echo time of 67 ms; field of view (FOV) of 192 mm \times 192 mm; b value of 0 and 1000 s/mm²; slice thickness of 4.5 mm; spacing between slices of 5 mm; gradient directions of x, y, and z. ADC maps were derived with a mono-exponential model on the Philips Medical Systems workstation. The unit of ADC is 1×10^{-6} mm²/s.

Image segmentation was undertaken using the "Segment Editor" module of the open-source software 3D Slicer (www.slicer.org/). Manual segmentation was undertaken by a radiologist who had 5 years of experience with head-and-neck imaging. ROIs were delineated manually to cover the whole tumor as much as possible (**Fig. 1**). Visible necrotic and cystic components within the tumor were excluded by referencing T2WI and contrast-enhanced T1WI. To verify the reproducibility of inter-observer delineation, 50 patients were selected randomly, and then another radiologist with 10 years of experience in head-and-neck imaging analyzed these images independently. The intraclass correlation coefficient (ICC) was used to determine agreement in the measurement of radiomics features. We selected an ICC ≥ 0.75 to denote "acceptable reliability".

Extraction of radiomics features was conducted using the "Radiomics" module of 3D Slicer, which is based on an open-source python package: Pyradiomics (www.radiomics.io/pyradiomics.html). The radiomics features comprised the following features: (i) size and shape; (ii) first-order histogram; (iii)

texture; (iv) wavelet. The texture features included the gray-level co-occurrence matrix (GLCM), gray-level run length matrix (GLRLM). The wavelet features were namely the recalculated histogram and textural features after wavelet decomposition in three directions (x, y, z) of the original images. Details about radiomics features have been interpreted at <https://pyradiomics.readthedocs.io/en/latest/features.html>.

Statistical analyses

All statistical analyses were conducted using R software (www.r-project.org). The reported statistical significance levels are all two-sided, and significance was set at 0.05. The age, gender, maximum diameter and tumor grading between training and testing cohorts were compared by the independent-sample *t*-test or chi-square test, respectively. The association of radiomics features or radiomics signature with histologic grade was analyzed using the Mann-Whitney *U*-test.

Construction and validation of the radiomics signature

Considering the high complexity of radiomics features, there was a risk of overfitting in the analysis. The least absolute shrinkage and selection operator (LASSO) logistic regression model was used in the training cohort to identify the most valuable predictive features and build a radiomics signature. It could minimize the binomial deviance by selection of a tuning parameter (λ), which adopted ten-fold cross-validation with minimum criteria in our study[15]. Simultaneously, a formula was generated using a linear combination of the optimal features weighted by their respective coefficients. The radiomics score for each patient was calculated based on this formula. Analyses of receiver operating characteristics (ROC) curves were done to assess the predictive ability of radiomics features and the radiomics signature, and the area under the ROC curve (AUC) was obtained. The optimal cutoff value of the radiomics signature determined in the training cohort was applied to the testing cohort to derive the accuracy, sensitivity and specificity.

Results

Patient characteristics

Patient characteristics in training and testing cohorts are listed in Table 1. The training cohort comprised 63 patients: 45 had a low-grade, 18 had a high-grade tumor. The testing cohort comprised 32 patients: 21 had a low-grade, 11 had a high-grade tumor. No significant differences were found between training and testing cohorts in terms of age ($P = 0.665$), gender ($P = 0.451$), maximum diameter ($P = 0.472$) and tumor grading ($P = 0.730$). **Construction and validation of radiomics signature**

In total, we extracted 526 radiomics features from ADC maps. After robustness assessment, 437 features with an ICC ≥ 0.75 remained. Of these features, 143 features were identified to be associated significantly with tumor grading (low-grade vs. high-grade). There was no significant difference in mean ADC on original images between low and high-grade tumors ($P = 0.862$).

Six optimal features were selected by LASSO regression (**Fig. 2**). The weighting coefficients of these features used to calculate radiomics score are shown in **Table 2**. Of those radiomics features, Original_Histogram_Skewness ($P = 0.016$), wLLH_Histogram_Entropy ($P = 0.002$), wLLH_GLRLM_RunEntropy ($P = 0.002$), wHHH_GLCM_InverseVariance ($P = 0.012$), and wHHL_GLCM_Correlation ($P = 0.002$) were significantly higher in high-grade than in low-grade, and wHHL_Histogram_90Percentile ($P = 0.004$) was significantly higher in low-grade than in high-grade (**Table 2**). The AUCs of the optimal features were ranging from 0.69 to 0.76 and the wLLH_Histogram_Entropy achieved the best performance (**Fig. 3 and Table 2**).

The radiomics score showed a significant difference between low- and high-grade tumors in training ($P < 0.001$) and testing ($P = 0.012$) cohorts, with the former being much higher (**Fig. 4**). The radiomics signature yielded an AUC of 0.82 in the training cohort and 0.78 in the testing cohort (**Fig. 3**). On the basis of the cutoff value obtained from the training cohort, the ADC-based radiomics signature achieved a favorable classification performance, which yielded accuracies of 0.75 and 0.78, sensitivities of 0.71 and 0.86, and specificities of 0.83 and 0.64 in the training and testing cohorts, respectively (**Fig. 4, Table 3**).

Discussion

In the present study we developed and validated an ADC-based radiomics signature for predicting histologic grade in SCC of the tongue and MF. Based on a significant difference in the radiomics score, the radiomics signature could successfully differentiate between low- and high-grade tumors.

During pretreatment evaluation, the histologic grade of SCC of the tongue and MF has long been considered an important prognostic factor following the TNM stage independently or with other biomarkers[7, 16]. Invasive biopsy is the “gold standard” for pretreatment evaluation of histologic grade, but is often limited due to sample bias[17]. As a non-invasive approach for characterizing tumors comprehensively, ADC-based radiomics has demonstrated potential for prediction of the histologic grade of glioma[18], cervical cancer[19], and bladder cancer[20]. Therefore, we investigated the predictive ability of radiomics features from ADC maps for the histologic grade of SCCs of the tongue and MF.

In this study, a supervised LASSO method was used to construct a radiomics signature for predicting histologic grade, which could provide comprehensive information about tumor heterogeneity. This method is designed to avoid overfitting for analyzing large numbers of radiomics features with a relatively small sample size, and has been used widely in radiomics research [21, 22]. 231 candidate features associated with histologic grade were reduced to six potential predictors to build an ADC-based radiomics signature. The signature showed a significant difference between low- and high-grade tumors in both cohorts, and performed well for predicting histologic grade, with an AUC of 0.82 for the training cohort and 0.78 for the testing cohort. Ahn et al.[8] reported that the mean ADC from a high b-value (2000 s/mm²) DWI had an accuracy of 0.70 for distinguishing low- and high-grade head-and-neck SCCs, but was not validated. In our work, on the basis of the cutoff values from the training cohort, the radiomics signature could differentiate between low- and high-grade tumors in the testing cohort with an accuracy

of 0.78, which suggested that the ADC-based radiomics signature outperformed the measurement of mean ADC from DWI with high b value. Given the comparable proportions of low- and high-grade tumors in both cohorts, the similar predictive performance implied that the radiomics signature was robust. If our study data can be reproduced from other centers, our results would likely suggest that an ADC-based radiomics signature could be used for computer-aided grading of SCCs of the tongue and MF.

In agreement with previous studies [6, 8], mean ADC on original ADC maps with $b = 0$ and 1000 s/mm^2 was found to be not significantly different between low- and high-grade tumors. The more prevalent microscopic necrotic areas and peritumoral edema with an increased ADC value and absence of keratinization of cells known to hinder water diffusion would explain (at least in part) the higher-than-expected ADC in high-grade tumors [8]. Of the optimal radiomics features, positive skewness on original ADC maps was demonstrated in low- and high-grade tumors, and was significantly greater in the latter. Skewness indicates the asymmetry of the histogram distribution, with a higher positive skew denoting that the voxel values cluster toward the lower end of the histogram [23]. Studies have reported significantly higher ADC skewness in high- than low-stage renal cell carcinomas [24], as well as malignant compared with benign endometrial tumors [23]. Our observation of higher ADC skewness within high-grade SCCs of the tongue and MF reflected a predominance of lower ADC values resulting from neoplasia-related cellularity. In addition, Histogram_Entropy, GLRLM_RunEntropy, GLCM_InverseVariance, and GLCM_Correlation of ADC maps after wavelet decomposition were significantly higher in high-grade than in low-grade tumors. The histogram, GLCM, and GLRLM are typical first-, second- and high-order descriptions of the pixel distribution within a ROI, and can characterize the global, local, and regional heterogeneity of tumors on different scales [25]. Presumably, these findings reflect the fact that high-grade tumors have greater intratumoral heterogeneity than low-grade tumors resulting from increased hypoxic voids, necrosis, and edema within the tumor.

The present study had four main limitations. First, this single-center study was relatively small, and multicenter researches with larger patient cohorts are needed to confirm our findings. Second, Grade-II and Grade-III tumors were not analyzed separately because of the small number of samples. Third, delineating the whole tumor volume was challenging because some tumors were infiltrative with indistinct borders. Fourth, the possibility of type-I errors >0.05 could not be avoided without adoption of multiple-testing correction. However, given the small sample size and exploratory purpose of our preliminary study, multiple-testing correction would not have been appropriate[26].

Conclusions

Our preliminary study demonstrated that an ADC-based radiomics signature showed satisfactory performance in tumor grading of SCCs of the tongue and MF, and could assist physicians to make a clinical diagnosis.

Abbreviations

SCC: squamous cell carcinoma; MF: mouth floor; DWI: diffusion-weighted imaging; ADC: apparent diffusion coefficient; ROI: region of interest; TNM: tumor-node-metastasis; MRI: magnetic resonance imaging; T1WI: T1-weighted imaging; T2WI: T2-weighted imaging; FOV: field of view; ICC: intraclass correlation coefficient; GLCM: gray-level co-occurrence matrix; GLRLM: gray-level run length matrix; LASSO: least absolute shrinkage and selection operator; ROC: receiver operating characteristics; AUC: area under the curve

Declarations

Ethics approval and consent to participate

The study was approved by Institutional Review Board of Shanghai Ninth People's Hospital. Due to the retrospective study design individual consent was waived.

Consent for publication

Not applicable.

Availability of data and material

The dataset supporting the conclusions of this article is available upon request to the corresponding author.

Competing interests

The authors declare that they have no competing interests.

Funding

This work was supported by funds from the National Scientific Foundation of China (91859202, 81771901)

Authors' contributions

XT and JR conceived and designed the study. JR, YY and YS collected the data. JR and MQ analyzed the data and wrote the paper. All authors read and approved the final manuscript for publication.

Acknowledgements

Not applicable.

References

1. Shah JP and Gil Z. Current concepts in management of oral cancer–surgery. *Oral Oncol.* 2009;45:394-401.
2. Zhang T, Lubek JE, Salama A, et al. Treatment of cT1N0M0 tongue cancer: outcome and prognostic parameters. *J Oral Maxillofac Surg.* 2014;72:406-14.
3. Jerjes W, Upile T, Petrie A, et al. Clinicopathological parameters, recurrence, locoregional and distant metastasis in 115 T1-T2 oral squamous cell carcinoma patients. *Head Neck Oncol.* 2010;2:9.
4. Kademani D, Bell RB, Bagheri S, et al. Prognostic factors in intraoral squamous cell carcinoma: the influence of histologic grade. *J Oral Maxillofac Surg.* 2005;63:1599-605.
5. Thomas B, Stedman M, and Davies L. Grade as a prognostic factor in oral squamous cell carcinoma: a population-based analysis of the data. *Laryngoscope.* 2014;124:688-94.
6. Bonello L, Preda L, Conte G, et al. Squamous cell carcinoma of the oral cavity and oropharynx: what does the apparent diffusion coefficient tell us about its histology? *Acta Radiol.* 2016;57:1344-51.
7. Yun TJ, Kim JH, Kim KH, et al. Head and neck squamous cell carcinoma: differentiation of histologic grade with standard- and high-b-value diffusion-weighted MRI. *Head Neck.* 2013;35:626-31.
8. Ahn SJ, Choi SH, Kim YJ, et al. Histogram analysis of apparent diffusion coefficient map of standard and high B-value diffusion MR imaging in head and neck squamous cell carcinoma: a correlation study with histological grade. *Acad Radiol.* 2012;19:1233-40.
9. Gillies RJ, Kinahan PE, and Hricak H. Radiomics: Images Are More than Pictures, They Are Data. *Radiology.* 2016;278:563-77.
10. Ren J, Tian J, Yuan Y, et al. Magnetic resonance imaging based radiomics signature for the preoperative discrimination of stage I-II and III-IV head and neck squamous cell carcinoma. *Eur J Radiol.* 2018;106:1-6.
11. Zhang B, Ouyang F, Gu D, et al. Advanced nasopharyngeal carcinoma: pre-treatment prediction of progression based on multi-parametric MRI radiomics. *Oncotarget.* 2017;8:72457-65.
12. Huang Yq, Liang Ch, He L, et al. Development and Validation of a Radiomics Nomogram for Preoperative Prediction of Lymph Node Metastasis in Colorectal Cancer. *Journal of Clinical Oncology.* 2016;34:2157-64.
13. Buch K, Fujita A, Li B, et al. Using Texture Analysis to Determine Human Papillomavirus Status of Oropharyngeal Squamous Cell Carcinomas on CT. *AJNR Am J Neuroradiol.* 2015;36:1343-8.
14. Vallieres M, Kay-Rivest E, Perrin LJ, et al. Radiomics strategies for risk assessment of tumour failure in head-and-neck cancer. *Sci Rep.* 2017;7:10117.

15. Tibshirani R. Regression shrinkage and selection via the lasso: a retrospective. *Journal of the Royal Statistical Society*. 2011;73:273-82.
16. Fortin A, Couture C, Doucet R, et al. Does histologic grade have a role in the management of head and neck cancers? *J Clin Oncol*. 2001;19:4107-16.
17. Dik EA, Ipenburg NA, Kessler PA, et al. The value of histological grading of biopsy and resection specimens in early stage oral squamous cell carcinomas. *J Craniomaxillofac Surg*. 2018;46:1001-6.
18. Wang Q, Li Q, Mi R, et al. Radiomics Nomogram Building From Multiparametric MRI to Predict Grade in Patients With Glioma: A Cohort Study. *J Magn Reson Imaging*. 2019;49:825-33.
19. Liu Y, Zhang Y, Cheng R, et al. Radiomics analysis of apparent diffusion coefficient in cervical cancer: A preliminary study on histological grade evaluation. *J Magn Reson Imaging*. 2019;49:280-90.
20. Zhang X, Xu X, Tian Q, et al. Radiomics assessment of bladder cancer grade using texture features from diffusion-weighted imaging. *J Magn Reson Imaging*. 2017;46:1281-8.
21. Zhu X, Dong D, Chen Z, et al. Radiomic signature as a diagnostic factor for histologic subtype classification of non-small cell lung cancer. *Eur Radiol*. 2018;28:2772-8.
22. Wu L, Wang C, Tan X, et al. Radiomics approach for preoperative identification of stages I-II and III-IV of esophageal cancer. *Chin J Cancer Res*. 2018;30:396-405.
23. Kierans AS, Doshi AM, Dunst D, et al. Retrospective Assessment of Histogram-Based Diffusion Metrics for Differentiating Benign and Malignant Endometrial Lesions. *J Comput Assist Tomogr*. 2016;40:723-9.
24. Kierans AS, Rusinek H, Lee A, et al. Textural differences in apparent diffusion coefficient between low- and high-stage clear cell renal cell carcinoma. *AJR Am J Roentgenol*. 2014;203:W637-44.
25. Liu Y, Xu X, Yin L, et al. Relationship between Glioblastoma Heterogeneity and Survival Time: An MR Imaging Texture Analysis. *AJNR Am J Neuroradiol*. 2017;38:1695-701.
26. Rothman KJ. No adjustments are needed for multiple comparisons. *Epidemiology*. 1990;1:43-6.

Tables

Table 1 Baseline characteristics of patients in training and testing cohorts

Characteristics	Training cohort (N=63)	Testing cohort (N=32)	<i>P</i>
Age	55.7±13.2	57.4±14.0	0.665
Gender (N [%])			0.451
Male	40 (63.5)	17 (53.1)	
Female	23 (36.5)	15 (46.9)	
Maximum diameter (mm)	32.9±14.4	30.8±13.4	0.472
Tumor grading (N [%])			0.73
Low-grade	45 (71.4)	21 (65.6)	
High-grade	18 (28.6)	11 (34.4)	

Age and maximum diameter are expressed as the mean ± standard deviation.

Table 2 Optimal features for predicting histologic grade

Parameter	Low-grade	High-grade	<i>P</i>	AUC	LASSO coefficient
Original_Histogram_Skewness	0.53(0.10-0.87)	0.88(0.52-1.15)	0.016	0.69	-0.073
wLLH_Histogram_Entropy	5.71(5.35-5.96)	6.04(5.92-6.29)	0.002	0.76	-0.663
wLLH_GLRLM_RunEntropy	5.79(5.41-6.08)	6.12(6.01-6.32)	0.002	0.75	-0.032
wHHH_GLCM_InverseVariance	0.44(0.39-0.47)	0.46(0.44-0.48)	0.012	0.71	-0.211
wHHL_GLCM_Correlation	0.04(0.01-0.06)	0.07(0.05-0.09)	0.002	0.75	-2.711
wHHL_Histogram_90Percentile	41.42(35.32-51.46)	35.18(32.00-36.92)	0.004	0.74	0.003
(Intercept)					5.095

Data are the median (interquartile range).

AUC area under the curve, *LASSO* least absolute shrinkage and selection operator.

Table 3 Predictive performance of the radiomics signature in the training and testing cohorts

Data	AUC (95%CI)	Sensitivity	Specificity	NPV	PPV	Accuracy
Training cohort	0.82(0.71-0.93)	0.71	0.83	0.91	0.54	0.75
Testing cohort	0.78(0.60-0.95)	0.86	0.64	0.82	0.70	0.78

AUC area under the curve, *CI* confidence interval, *NPV* negative predictive value, *PPV* positive predictive value

Figures

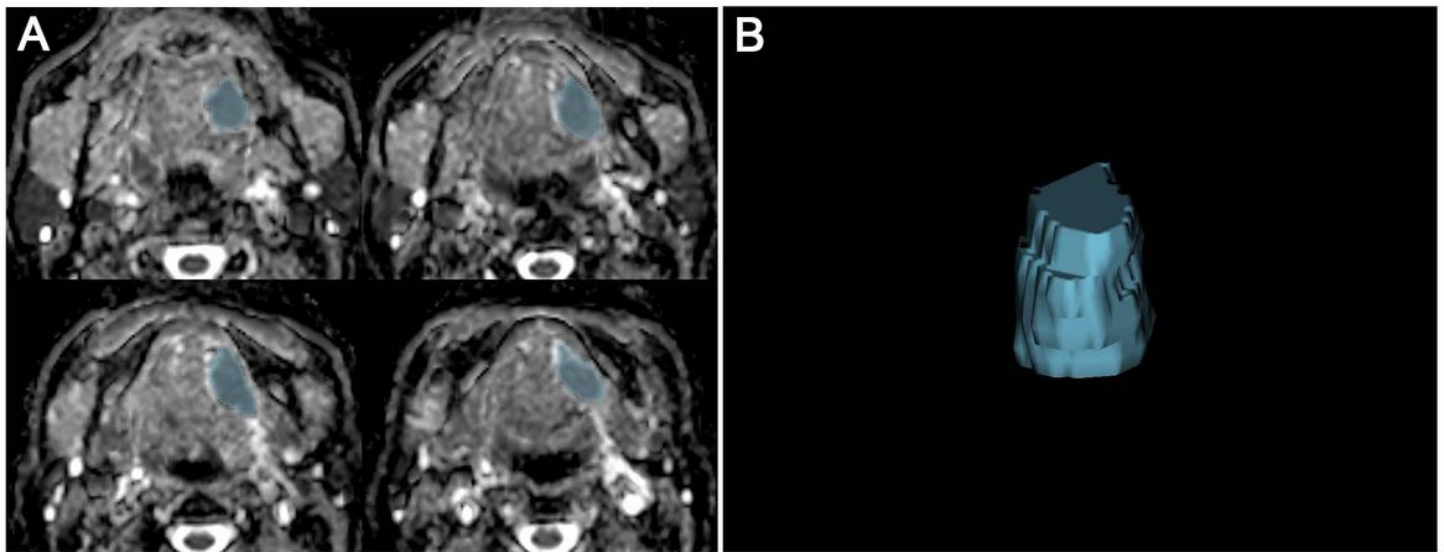


Figure 1

Image segmentation. a: ADC maps of $b = 0$ and 1000 s/mm^2 . b: whole-tumor region of interest

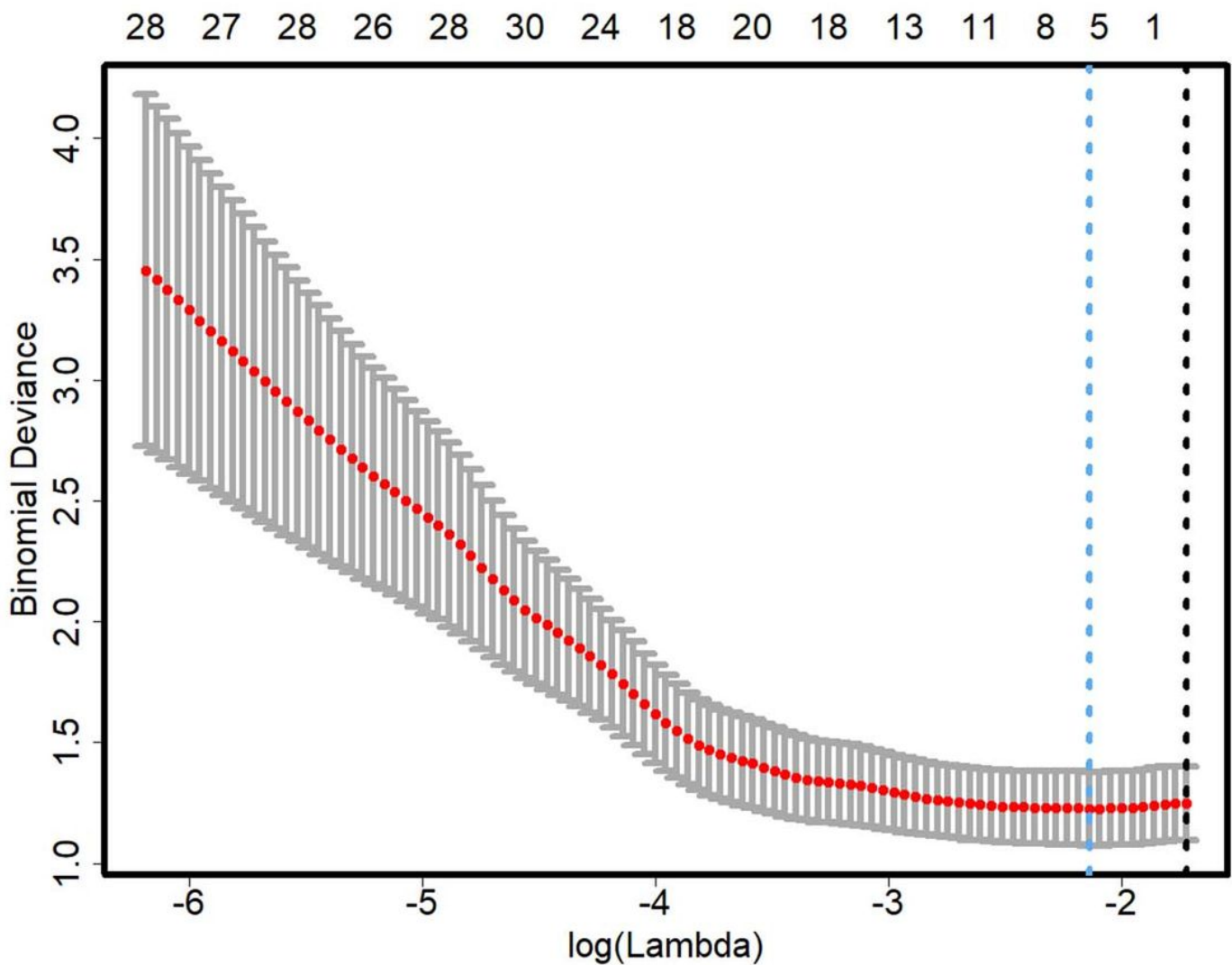


Figure 2

Feature selection using the least absolute shrinkage and selection operator (LASSO) binary regression model. Tuning parameter (λ) selection in the LASSO model by ten-fold cross-validation with the minimum criteria. Dotted vertical lines were drawn at the optimal values by using the minimum criteria (blue line) and the 1 standard error of the minimum criteria (the 1-SE criteria, black line)

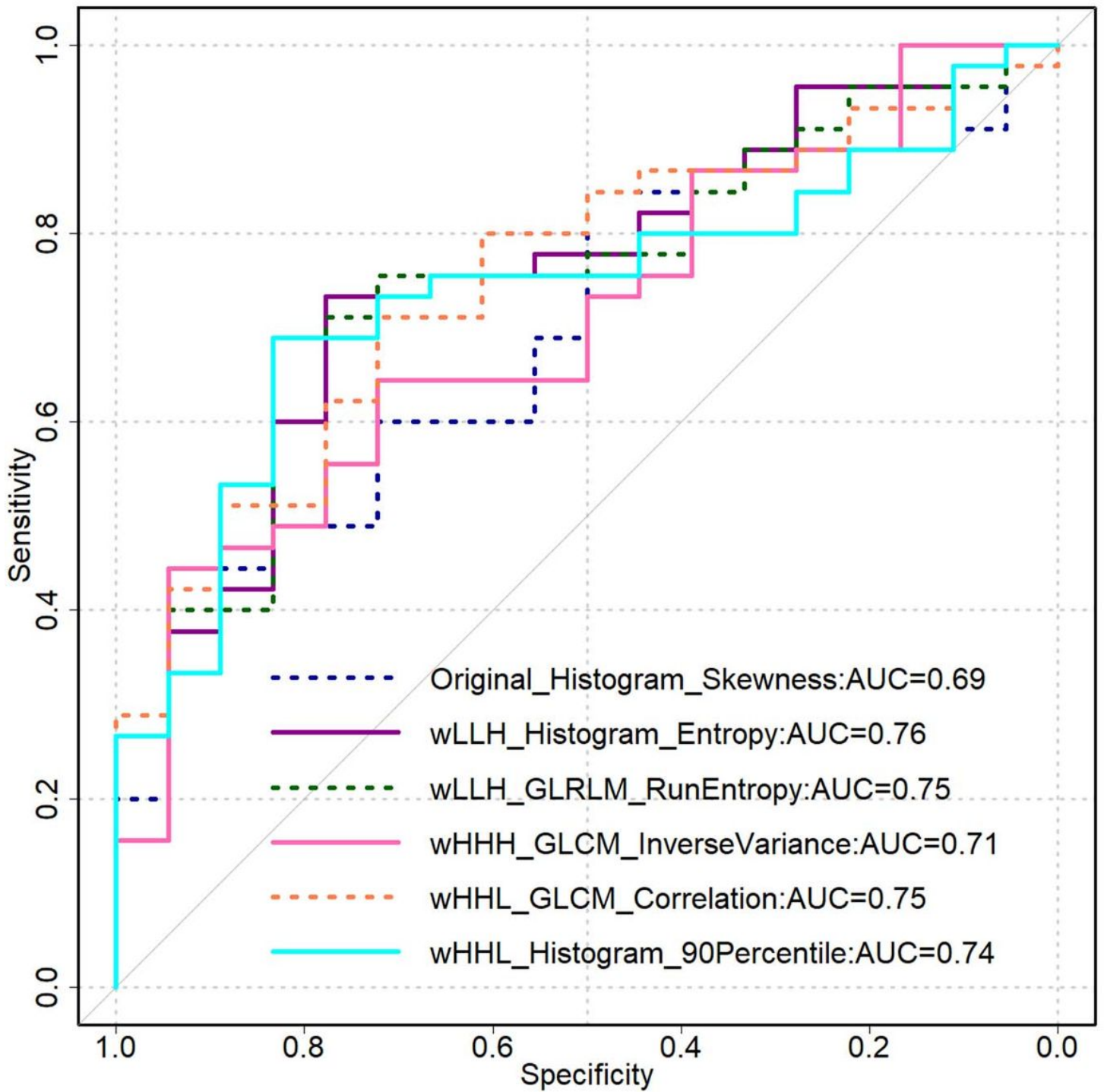


Figure 3

Receiver operating characteristic (ROC) curves of the optimal features for discriminating between low- and high-grade in the training cohort.

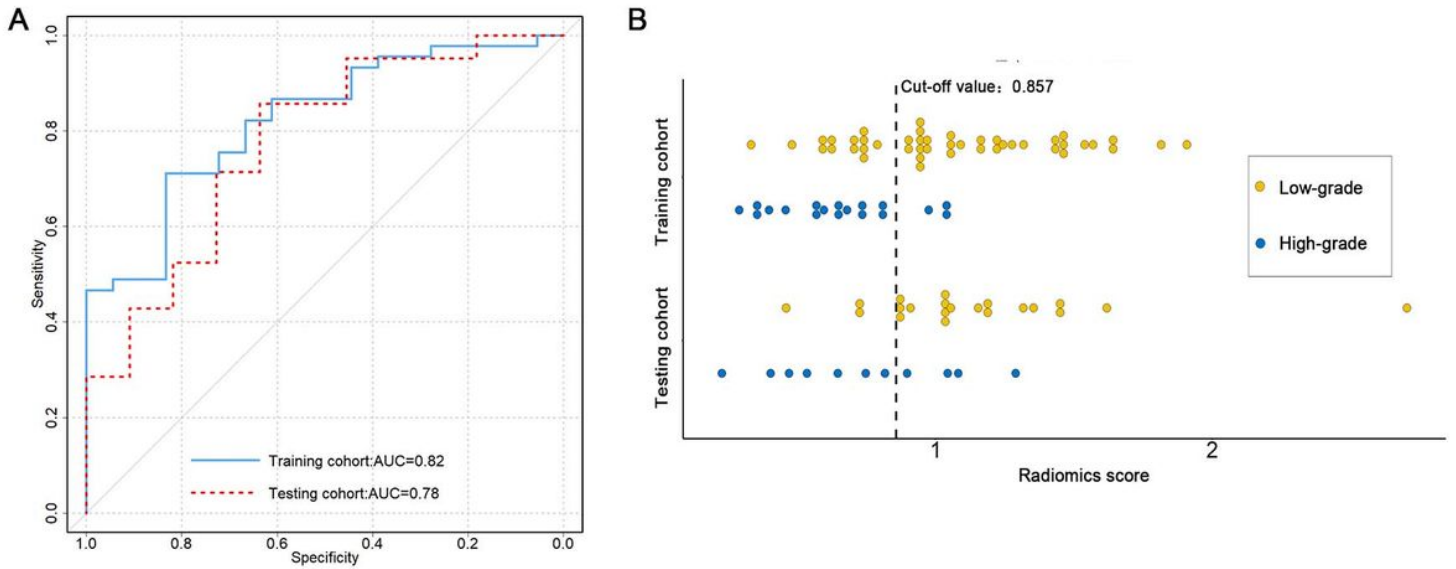


Figure 4

The predictive performance for radiomics signature. A: ROC curves for the radiomics signature in the training and testing cohorts. B: each patient with regard to the classification of tumor grade in the training and testing cohorts.